ZOOLOGICAL RESEARCH

MOSPD2 is a receptor mediating the LEAP-2 effect on monocytes/macrophages in a teleost, *Boleophthalmus pectinirostris*

Chang-Hong Li[1,2,3,#], Jie Chen[2,4,#], Li Nie[1], Jiong Chen[1,2,3,*]

[1] *State Key Laboratory for Managing Biotic and Chemical Threats to the Quality and Safety of Agro-Products*, *Ningbo University*, *Ningbo*, *Zhejiang* 315211, *China*

[2] *Laboratory of Biochemistry and Molecular Biology*, *School of Marine Sciences*, *Meishan Campus*, *Ningbo University*, *Ningbo*, *Zhejiang* 315832, *China*

[3] *Key Laboratory of Applied Marine Biotechnology of Ministry of Education*, *Meishan Campus*, *Ningbo University*, *Ningbo*, *Zhejiang* 315832, *China*

[4] *College of Ecology*, *Lishui University*, *Lishui*, *Zhejiang* 323000, *China*

ABSTRACT

Liver-expressed antimicrobial peptide 2 (LEAP-2) is a cationic peptide that plays an important role in a host's innate immune system. We previously demonstrated that mudskipper (*Boleophthalmus pectinirostris*) LEAP-2 (BpLEAP-2) induces chemotaxis and activation of monocytes/ macrophages (MO/MΦ). However, the molecular mechanism by which BpLEAP-2 regulates MO/MΦ remains unclear. In this study, we used yeast two-hybrid cDNA library screening to identify mudskipper protein(s) that interacted with BpLEAP-2, and characterized a sequence encoding motile sperm domain-containing protein 2 (BpMOSPD2). The interaction between BpLEAP-2 and BpMOSPD2 was subsequently confirmed by co-immunoprecipitation (Co-IP). Sequence analyses revealed that the predicted BpMOSPD2 contained an N-terminal extracellular portion composed of a CRAL-TRIO domain and a motile sperm domain, a C-terminal transmembrane domain, and a short cytoplasmic tail. Phylogenetic tree analysis indicated that BpMOSPD2 grouped tightly with fish MOSPD2 homologs and was most closely related to that of the Nile tilapia (*Oreochromis niloticus*). The recombinant BpMOSPD2 was produced by prokaryotic expression and the corresponding antibody was prepared for protein concentration determination. RNA interference was used to knockdown *BpMOSPD2* expression in the mudskipper MO/MΦ, and the knockdown efficiency was confirmed by quantitative real-time polymerase chain reaction (qRT-PCR) and western blotting. Knockdown of *BpMOSPD2* significantly inhibited BpLEAP-2-induced chemotaxis of mudskipper MO/MΦ and BpLEAP-2-induced bacterial killing activity. Furthermore, knockdown of *BpMOSPD2* inhibited the effect of BpLEAP-2 on mRNA expression levels

Received: 01 August 2020; Accepted: 10 October 2020; Online: 11 October 2020

Foundation items: This project was supported by the National Natural Science Foundation of China (31972821, 31772876), Zhejiang Provincial Natural Science Foundation of China (LZ18C190001), Scientific Innovation Team Project of Ningbo (2015C110018), and K.C. Wong Magna Fund in Ningbo University

[#]Authors contributed equally to this work

*Corresponding author, E-mail: chenjiong@nbu.edu.cn

DOI: 10.24272/j.issn.2095-8137.2020.211

of *BpIL-10*, *BpTNFα*, *BpIL-1β*, and *BpTGFβ* in MO/MΦ. In general, BpMOSPD2 directly interacted with BpLEAP-2, and mediated the effects of BpLEAP-2 on chemotaxis and activation of mudskipper MO/MΦ. This is the first identification of MOSPD2 as a receptor for LEAP-2.

Keywords: LEAP-2; Monocyte/macrophage; MOSPD2; RNA interference; Yeast two-hybrid

INTRODUCTION

Host defense peptides (HDPs), also known as antimicrobial peptides, are typically short (18–46 amino acids, aa), usually cationic, amphipathic peptides that defend the host against various pathogens (Hancock et al., 2016). The antimicrobial effects of HDPs are mediated by their ability to interact directly with bacterial membrane-associated protein targets that induce cell membrane damage or penetrate the bacterial cytoplasm to interact with intracellular targets and induce cell damage (Brogden, 2005; Hale & Hancock, 2007). HDPs possess a broad range of immunomodulatory functions that promote bacterial clearance and induction of chemotaxis, phagocytosis, and cytokine production of immune cells (Brown & Hancock, 2006; Fruitwala et al., 2019; Hancock et al., 2012; Rajanbabu & Chen, 2011; Röhrl et al., 2010; Wu et al., 2018). Defensins and cathelicidins are the most well-characterized HDPs in mammals (Fabisiak et al., 2016; Fruitwala et al., 2019). Human β-defensins (β-defensin 2 and β-defensin 3) can chemoattract immune cells, induce cytokines/chemokines, and modulate cellular functions and differentiation/activation markers through different receptors, such as C-C motif chemokine receptor 6 (CCR6), CCR4, CCR2, C-X-C motif chemokine receptor 4, Mas-related gene X2 receptor (MrgX2), and Gαi protein-coupled receptor (Fruitwala et al., 2019; Gupta et al., 2016; Röhrl et al., 2010). Cathelicidins (LL-37) interact with a broad variety of receptors, such as formyl-peptide receptor-like 1 (FPRL1), FPRL2, CXCR2, purinergic ligand-gated ion channel 7 receptor (P2X7R), and MrgX2, and exhibit multifunctional immunomodulatory activities (Bąbolewska & Brzezińska-Błaszczyk, 2015; Scott et al., 2002; Subramanian et al., 2011; Vandamme et al., 2012).

Fish are a great source of HDPs, including defensins (Zhou et al., 2020; Zhu et al., 2017), cathelicidins (Li et al., 2015a; Lu et al., 2011), hepcidins (Chen et al., 2018), liver-expressed antimicrobial peptide 2 (LEAP-2) (Bo et al., 2019; Chen et al., 2016; Li et al., 2015b; Liu et al., 2020), piscidins (Yang et al., 2016; Zahran et al., 2019), and NK-lysin (Ding et al., 2019). Similar to their homologs in mammals, these HDPs not only directly kill microorganisms, but also exert immunoprotective effects on fish through their immunomodulatory functions, including induction of chemotaxis, phagocytosis, bacterial killing, and cytokine production of immune cells (Chen et al., 2016, 2018; Ding et al., 2019; Li et al., 2015a; Zhou et al., 2020). We recently confirmed that P2X7R mediates the immunomodulatory functions of cathelicidin in monocytes/macrophages (MO/MΦ) from ayu (*Plecoglossus altivelis*) (Li et al., 2015a), in accordance with that reported in mammals (Elssner et al., 2004; Nagaoka et al., 2006). However, information on the underlying mechanism in fish HDPs related to their immunomodulatory functions remains limited.

LEAP-2 is also a human blood-derived antimicrobial peptide with direct antimicrobial activities in human blood ultrafiltrates (Krause et al., 2003). In addition to its direct antimicrobial activities, LEAP-2 also exhibits other important biological functions. Due to its significantly lower expression in human immunodeficiency virus type 1 (HIV)- and hepatitis C virus (HCV)-infected patients compared with healthy donors, LEAP-2 is a key marker associated with immune activation (Shata et al., 2013). Furthermore, LEAP-2 is an endogenous ligand for the growth hormone secretagogue receptor (also known as the ghrelin receptor) in mice (Barrile et al., 2019; Ge et al., 2018). LEAP-2 homologs have also been identified in many teleosts and play important roles against pathogens (Chen et al., 2019; Li et al., 2014, 2015b; Liu et al., 2014; Luo et al., 2020). They generally exert direct bacterial killing activity to improve fish survival and decrease bacterial load (Li et al., 2014, 2015b). Interestingly, we previously found that mudskipper (*Boleophthalmus pectinirostri*s) LEAP-2 (BpLEAP-2) has no direct killing effect on *Edwardsiella tarda*, an intracellular bacterial pathogen of mudskippers, but can protect mudskippers against *E. tarda* by inducing the migration and activation of MO/MΦ (Chen et al., 2016). However, the mechanism by which BpLEAP-2 regulates MO/MΦ remains unclear. In the current study, we identified mudskipper protein(s) that interacted with BpLEAP-2 using yeast two-hybrid cDNA library screening. Motile sperm domain-containing protein 2 of the mudskipper (BpMOSPD2) was identified and its interaction was confirmed by co-immunoprecipitation (Co-IP). We subsequently investigated the influence of *BpMOSPD2* knockdown on chemotactic activity of BpLEAP-2 towards MO/MΦ, as well as the effects of BpLEAP-2 on mudskipper MO/MΦ functions, including bacterial killing and cytokine mRNA expression.

MATERIALS AND METHODS

Fish rearing

All experimental mudskipper fish, each weighing 30–35 g, were purchased from a commercial farm in Ningbo City, China. All fish were healthy without any pathological signs. They were temporarily kept in brackish water (salinity 10) tanks at 24–26 °C in a recirculating water system and acclimatized to laboratory conditions for two weeks before experiments. All experiments were performed according to the Experimental Animal Management Law of China and approved by the Animal Ethics Committee of Ningbo University.

Construction, autoactivation, and toxicity tests of bait plasmid

Total RNA was extracted from the livers of healthy

mudskippers using RNAiso reagent (TaKaRa, China). After treatment with DNase I (TaKaRa), first cDNA strand synthesis was carried out using AMV reverse transcriptase (TaKaRa). Two primers, i.e., LEAP-2-m1(+): 5'-CCGGAATTCATGAC CCCTCTCTGGAGGAT-3' (*Eco*R I site is underlined) and LEAP-2-m1(−): 5'-CGCGGATCCTCAGTTGGTGACAGAAAC GG-3' (*Bam*H I site is underlined), were used to amplify the sequence encoding the mature peptide (aa 55–100) of BpLEAP-2. The amplicons were subsequently digested with *Eco*R I and *Bam*H I (Takara) and ligated into the *Eco*R I-*Bam*H I-cleaved pGBKT7 vector (Clontech, USA) to construct the bait plasmid pGBKT7-BpLEAP-2. The pGBKT7-BpLEAP-2 plasmid and empty pGBKT7 vector were transformed into *Saccharomyces cerevisiae* Y2HGold (Clontech) to test the autoactivation and toxicity of the bait protein. Transformants were then grown on SD/-Trp, SD/-Trp/X-α-Gal (40 μg/mL X-α-Gal), and SD/-Trp/X-α-Gal/AbA (40 μg/mL X-α-Gal and 125 ng/mL Aureobasidin A) agar plates for 3–5 d. Only bait that lacked autoactivation and toxicity was used in Y2H screening.

Cell preparation

Kidney-derived MO/MΦ from mudskippers were isolated and cultured as reported previously (Guan et al., 2017; Shen et al., 2020). Briefly, fish kidney leukocyte-enriched fractions were obtained using Ficoll-Hypaque PREMIUM (1.077 g/mL) (GE Healthcare, USA). Non-adherent cells were removed by washing, and adherent cells were incubated in complete medium (RPMI 1640, 5% mudskipper serum, 5% fetal bovine serum (FBS; Gibco, Thermo Fisher Scientific, USA), 100 U/mL penicillin, 100 μg/mL streptomycin) at 24 °C with 5% CO_2. The HEK293T cells were maintained in Dulbecco's modified Eagle's medium (Biochrom AG, Germany) supplemented with 10% (v/v) FBS, 100 U/mL penicillin (Sangon Biotech, China), and 100 μg/mL streptomycin (Sangon Biotech) at 37 °C with 5% CO_2. The HEK293T cells were then seeded into 6-well plates to allow growth until 70%–90% confluence on the day of transfection.

Construction of mudskipper MO/MΦ cDNA library for Y2H

Total RNA was extracted from the cultured mudskipper MO/MΦ using an RNAqueous Kit (Ambion, USA). mRNA was isolated from total RNA using an Oligotex-dT_{30} (super) mRNA Purification Kit (TaKaRa) and used as a template for the synthesis of first-strand cDNA by reverse transcription. The mudskipper MO/MΦ cDNA library for Y2H was constructed according to the protocol described in the Make Your Own "Mate & Plate™" Library System User Manual (Clontech). In brief, primer CDS III (5'-ATTCTAGAGGCCGAGGCGGCC GACATG-d(T_{30})VN-3') (V=A, T, C, or G; N=A, C, or G) was used to initiate first-strand cDNA synthesis, and primer SMART III (5'-AAGCAGTGGTATCAACGCAGAGTGGCCATT ATGGCCGGG-3') served as a short, extended template at the 5'-end of mRNA. Double-stranded cDNA (dscDNA) was amplified by long-distance polymerase chain reaction (LD-PCR) with the 5' PCR primer (5'-TTCCACCCAAGCAGTG GTATCAACGCAGAGTGG-3') and 3' PCR primer (5'-GTATC GATGCCCACCCTCTAGAGGCCGAGGCGGCCGACA-3') using an Advantage 2 PCR Kit (Takara). The LD-PCR products were purified using a CHROMA SPIN™ TE-1000 Column (Takara) to remove fragments smaller than 400 bp. The purified dscDNA amplicons and pGADT7-Rec vector (*Sma* I-linearized) were co-transformed into yeast strain Y187 using the Yeastmaker™ Yeast Transformation System 2 (Clontech).

The inserts of the dscDNA amplicons were determined by PCR amplification with 5' and 3' PCR primers. PCR amplification was run on a Mastercycler Pro Gradient PCR System (Eppendorf AG, Germany) in a 25 μL reaction volume containing 1.0 μL template DNA, 1.0 μL 5' PCR primer, 1.0 μL 3' PCR primer, 0.25 μL *Ex Taq* (Takara), 2.5 μL 10× *Ex Taq* PCR buffer, 2.0 μL dNTP (2.5 mol/L each), and 17.25 μL sterile ddH_2O. The PCR amplification conditions were 95 °C for 2 min followed by 30 cycles at 95 °C for 30 s, 60 °C for 30 s, and 72 °C for 3 min, and final 72 °C for 10 min. The PCR products were electrophoresed on 1.0% agarose gel, stained with ethidium bromide (EtBr), and photographed under ultraviolet (UV) illumination (Ultra-Violet Products Ltd., USA),

cDNA library screening by yeast mating

To identify BpLEAP-2-interacting MO/MΦ protein(s), we screened the mudskipper MO/MΦ cDNA library by yeast mating. Mating between Y2HGold/pGBKT7-BpLEAP-2 and mudskipper MO/MΦ cDNA library was performed according to the Matchmaker Gold Yeast Two-Hybrid System User Manual (Clontech). After 24 h of mating, the mating yeasts were plated on SD/-Leu/-Trp supplemented with X-α-Gal and Aureobasidin A (DDO/X/A) agar plates, then cultured at 30 °C for 5 d. All blue colonies that grew on DDO/X/A were patched to high-stringency SD/-Ade/-Leu/-Trp/-His supplemented with X-α-Gal and Aureobasidin A (QDO/X/A) agar plates, then cultured for 5 d at 30 °C. Finally, 30 potential positive colonies were obtained through screening.

Rescuing prey plasmids and confirming interactions

The prey plasmids were obtained from the potential positive clones using an Easy Yeast Plasmid Isolation Kit (Clontech) and used to transform the *Escherichia coli* strain TG1 (Beyotime Institute of Biotechnology, China). Potential positive prey plasmids from the initial screening were transformed into the yeast strain Y187, and their autoactivation and toxicity were tested. After that, the Y187 cells transformed with each potential positive prey plasmid were used to mate with the Y2HGold cells transformed with pGBKT7-BpLEAP-2 bait plasmid or empty pGBKT7 vector, respectively. The mated yeast cells were then spread onto QDO/X/A agar plates. The Y2HGold cells transformed with the pGBKT7-53 or pGBKT7 vector were used to mate with the Y187 cells transformed with the pGADT7-T or pGADT7-lam vector. After culturing at 30 °C for 5 d, only the blue colonies that grew on QDO/X/A agar plates were identified as true positive candidates. Finally, the true positive candidates were sequenced using the T7 primer, and the sequences obtained were blasted against the National

Center for Biotechnology Information (NCBI) databases to obtain descriptions of the closest matches.

Sequence analysis of BpMOSPD2

The protein domain architecture was analyzed using the SMART program (http://smart.emblheidelberg.de/). Multiple alignments were conducted using the ClustalW program (http://clustalw.ddbj.nig.ac.jp/). Phylogenetic and molecular evolutionary analyses were conducted using MEGA v7.0 (Kumar et al., 2016). All *MOSPD2* sequences used in this study are listed in Supplementary Table S1. The grass carp (*Ctenopharyngodon idellus*) *MOSPD2* sequence was obtained by searching the genome database of grass carp at the official National Center for Gene Research website (http://www.ncgr.ac.cn/grasscarp/) (Wang et al., 2015).

Co-IP assay

Using the primer pair: MOSPD2-ECD(+): 5'-ATAAGAAT GCGGCCGCAATGGCT GAAGTTGAACAACACGGA-3' (*Not* I site is underlined) and MOSPD2-ECD(−): 5'-CCCAAGCTT CTTCTGCACCCAGAGACACGTG-3' (*Hind* III site is underlined), the sequence encoding the extracellular domain peptide of BpMOSPD2 was amplified, digested by *Not* I and *Hind* III (Takara), and inserted into the pcDNA3.1-Myc-His vector (Invitrogen, USA) to construct the eukaryotic expression plasmid pcDNA3.1-BpMOSPD2-Myc-His. Using the primer pair: BpLEAP-2-m2(+): 5'-ATAAGAATGCGGCCGC AATGACCCCTCTCTGGAGGAT-3' (*Not* I site is underlined) and BpLEAP-2-m2(−): 5'-CCCAAGCTTGTTGGTGACAGAA ACGGTTGC-3' (*Hind* III site is underlined), the sequence encoding the mature peptide of BpLEAP-2 was amplified, digested by *Not* I and *Hind* III, and inserted into pcDNA3.1-Flag-His (a kind gift from Prof. Zong-Ping Xia, Zhejiang University, China) to construct the eukaryotic expression plasmid pcDNA3.1-BpLEAP2-Flag-His. The two constructed plasmids for transfection were prepared at the endotoxin-free level using an EZNA™ Plasmid Midi Kit (Omega Bio-Tek, USA) according to the manufacturer's protocols and the correctness of insertion was confirmed by sequencing. The HEK293T cells were co-transfected with pcDNA3.1-BpMOSPD2-myc-His and pcDNA3.1-BpLEAP2-Flag-His, as described previously (Ren et al., 2019). The HEK293T cells transiently transfected with pcDNA3.1-BpLEAP-2-Flag-His were used as a control. At 48 h post-transfection, the supernatant was removed, and the cells were washed with serum-free buffer and treated with 500 μL of cell lysis buffer for western blotting and IP (Beyotime) with 1 mmol/L PMSF (Beyotime). The lysis products of cells were centrifuged at 14 000 *g* for 10 min at 4 °C to collect the supernatant and subsequently incubated with 5 μL Myc Tag Mouse Monoclonal Antibody (Myc Tag mAb, Beyotime) at 4 °C overnight. The next day, the supernatant was added with up to 20 μL of Pierce™ Protein G Agarose (Thermo Scientific), shaken at 4 °C for 4 h, and washed thrice in cold phosphate-buffered saline (PBS). The precipitants were denatured in loading buffer for analysis via western blotting using 12% sodium dodecyl sulfate polyacrylamide gel electrophoresis (SDS-PAGE). The primary Flag Tag Mouse Monoclonal Antibody (Flag Tag mAb, Beyotime) was diluted to 1:2 000. The horseradish peroxidase-labeled goat anti-mouse IgG secondary antibody (HRP-IgG, Beyotime) was diluted to 1: 5 000. The results were visualized via chemiluminescence using a BeyoECL Plus Kit (Beyotime).

Prokaryotic expression and polyclonal antibody preparation

The complete open reading frame (ORF) sequence of *BpMOSPD2* was amplified from a mudskipper MO/MΦ cDNA template with the primers MOSPD2p(+): 5'-GGAATTC ATGGCTGAAGTTGAACAACACGGAG-3' (*Eco*R I site is underlined) and MOSPD2p(−): 5'-CAAGCTTTCAAGATGG CCGCTGTTGACC-3' (*Hind* III site is underlined). The amplicons were digested by *Eco*R I and *Hind* III and inserted into the pET-30a vector (Novagen, Lisbon, Portugal) to construct the prokaryotic expression plasmid pET-30a-BpMOSPD2. The recombinant plasmid was transformed into *E. coli* BL21 (DE3) *pLys*S to express the target protein by isopropyl-β-D-1-thiogalactopyranoside (IPTG) induction. The recombinant protein was purified using a nickel-nitrilotriacetic acid (Ni-NTA) column (Qiagen, China) and used as an antigen to immunize mice to produce antisera, as reported previously (Ren et al., 2019; Shen et al., 2020).

qRT-PCR

Total RNA extraction, DNase I digestion, first-strand cDNA synthesis, and qRT-PCR were conducted as reported previously (Ren et al., 2019). Here, qRT-PCR was performed on an ABI-StepOne Real-Time PCR System (Applied Biosystems, USA) using SYBR *premix Ex Taq* II (Takara). The primers used for qRT-PCR are listed in Table 1. The qRT-PCR amplification conditions were: 95 °C for 5 min; 40 cycles at 95 °C for 30 s, and 60 °C for 30 s; followed by melting curve analysis at 95 °C for 5 s, 65 °C for 15 s, and 95 °C for 15 s. Relative gene expression was calculated using the $2^{-\Delta\Delta CT}$ method (Livak & Schmittgen, 2001). The data were normalized against *Bp18S rRNA*. Each qRT-PCR run was performed with four samples and repeated three times.

RNA interference

RNA interference was conducted to knock down the expression of *BpMOSPD2* in MO/MΦ. *BpMOSPD2* siRNA (5'-CCGAGGCAAUCAGCAAACUCAGAUU-3') and scrambled siRNA (5'-CCGAACGGACUAAACACUCGGAAUU-3') were designed and synthesized (Invitrogen). The transfection of siRNA was performed using a Lipofectamine RNAiMAX reagent (Invitrogen) according to the manufacturer's protocols. Briefly, 5 μL of Lipofectamine RNAiMAX in 250 μL of Opti-MEM (Invitrogen) was mixed with 100 pmoL siRNA in 250 μL of Opti-MEM. The mixture was then incubated for 20 min at room temperature before addition to MO/MΦ at a final siRNA concentration of 40 nmol/L. Media were changed to complete media after 5.5 h of incubation, and cells were harvested after another 72 h of culture and preserved at −80 °C for subsequent qRT-PCR and western blot analysis of the

Table 1 Oligonucleotide primers used for qRT-PCR in this study

Primer	Gene	GenBank accession No.	Nucleotide sequence (5'–3')	Ampliconsize (bp)
MOSPD2-t(+)	*BpMOSPD2*	XM_020939150	GAGCCAGGAAACCAGAGACT	141
MOSPD2-t(−)			CCACTATCTCCACCGATGCT	
IL-1β-t(+)	*BpIL-1β*	KX492895	ACGAGTGGTGAATGTGGTCA	163
IL-1β-t(−)			GAACTGAGGTTGTGCTGCAA	
TNFα-t(+)	*BpTNFα*	KX492896	GGACAACAACGAGATCGTGA	155
TNFα-t(−)			GTTCCACCGTGTGACTGATG	
IL-10-t(+)	*BpIL-10*	XM_020936977	GTGGAGGGGTTCCCTCTAAG	179
IL-10-t(−)			GTGCGGAGGTAAAAGCTCAG	
TGFβ-t(+)	*BpTGFβ*	XM_020928521	TCAAAGGACACTTGCACAGC	183
TGFβ-t(−)			CAGGGCCAAGATCTGTGAAT	
18S rRNA-t(+)	*Bp18S rRNA*	KX492897	GGCCGTTCTTAGTTGGTGGA	112
18S rRNA-t(−)			CCCGGACATCTAAGGGCATC	
gyrB-t(+)	*gyrB*	FJ158597	TGGCGACACCGAGCAGA	207
gyrB-t(−)			ACAAACGCCTTAATCCCACC	

BpMOSPD2 gene and protein expression levels in mudskipper MO/MΦ, respectively. For qRT-PCR, the primer pair MOSPD2-t(+) and MOSPD2-t(−), which are specific to *BpMOSPD2*, was used (Table 1). Amplification and data analysis were the same as that described in the qRT-PCR section above. For western blot analysis, the polyclonal antibody of BpMOSPD2 (1:1 000) (for BpMOSPD2) and monoclonal antibody of mouse β-actin (1:1 000, Beyotime) (for mudskipper β-actin, Bpβ-actin) were used as the primary antibodies, with HRP-IgG (Beyotime) used as the secondary antibody. The results were visualized via chemiluminescence using a BeyoECL Plus Kit (Beyotime) and quantified using NIH ImageJ software. Relative band intensity of BpMOSPD2 was normalized against Bpβ-actin.

Chemotaxis assay

The chemotaxis assay was conducted as described previously (Chen et al., 2016). Mudskipper MO/MΦ cells were transfected with *BpMOSPD2* siRNA or scrambled siRNA for 72 h. After siRNA transfection, the adherent cells were loosened using trypsin-EDTA (0.05% Trypsin, Invitrogen) for 5 min and then centrifuged at 400 *g* for 5 min. The cells were resuspended in RPMI 1640 supplemented with 10% FBS and added to the upper chamber. BpLEAP-2 was added at 0 or 10.0 μg/mL to the lower Transwell chamber. After incubation at 24 °C for 4 h, the cells that migrated to the lower chamber were stained with Wright-Giemsa stain and counted under a light microscope (Nikon, Japan) at a magnification of 40×10. Each migration assay was performed in quadruplicate, and the percentage of cells that migrated to the lower chamber was calculated.

Bacterial killing assay

The bacterial killing assay was performed as described previously (Shen et al., 2020). Briefly, *E. tarda* cells in the logarithmic phase of growth were harvested, washed, resuspended, and adjusted to a final concentration of 2×10^7 colony forming units (CFU)/mL in sterile PBS. Mudskipper MO/MΦ cells were transfected with scrambled siRNA or *BpMOSPD2* siRNA for 72 h and then with 10 μg/mL BpLEAP-2 treatment for another 8 h. After washing with sterile PBS, the cells were infected with live *E. tarda* at an MOI of 10. Bacterial phagocytosis was allowed to proceed for 30 min at 24 °C in a 5% CO_2 atmosphere, and noninternalized *E. tarda* cells were removed by washing with sterile PBS. Samples of the uptake group were collected for RNA extraction, while samples of the kill group were further incubated for 1.5 h for bacterial killing before RNA extraction. Cells were subjected to RNA isolation and subsequent qRT-PCR detection for *E. tarda* using primers gyrB-t(+) and gyrB-t(−) (Table 1), which are specific to the *E. tarda DNA gyrase subunit B* (*gyrB*) gene (Shen et al., 2020). The Ct values obtained were used to calculate total CFUs/mL in all samples based on standard curves. Bacterial survival was determined by dividing the CFUs of the kill group by that of the uptake group.

Cytokine mRNA expression analysis

The mRNA expression changes in *tumor necrosis factor α* (*BpTNFα*), *interleukin 1β* (*BpIL-1β*), *interleukin 10* (*BpIL-10*), and *transforming growth factor β* (*BpTGFβ*) in mudskipper MO/MΦ were determined by qRT-PCR. Briefly, mudskipper MO/MΦ cells were transfected with scrambled siRNA or *BpMOSPD2* siRNA for 72 h and then with 10 μg/mL BpLEAP-2 treatment for another 8 h. The cells were washed with sterile PBS, infected with live *E. tarda* at an MOI of 10, and harvested at 8 h post-treatment. Total RNA extraction from MO/MΦ, DNase I treatment, first-strand cDNA synthesis, and qRT-PCR analysis were performed as described above. The primer pairs specific to *BpTNFα*, *BpIL-1β*, *BpIL-10*, and *BpTGFβ* are listed in Table 1. The mRNA expression of the target gene was normalized to *Bp18S rRNA* mRNA expression.

Statistical analysis

All data are presented as mean±*SD*. Statistical analysis was conducted using one-way analysis of variance (ANOVA) with

SPSS v13.0 (SPSS Inc., USA). Statistical significance was considered at $P<0.05$.

RESULTS

Autoactivation and toxicity tests of bait plasmid pGBKT7-BpLEAP-2 in yeast

The bait plasmid pGBKT7-BpLEAP-2 was transformed into yeast Y2HGold cells to test the autoactivation and toxicity of the bait. The transformants were grown on SD/-Trp, SD/-Trp/X-α-Gal, and SD/-Trp/X-α-Gal/AbA plates. Y2HGold cells transformed with the pGBKT7-BpLEAP-2 plasmid grew as white colonies on the SD/-Trp and SD/-Trp/X-α-Gal plates, but did not grow on the SD/-Trp/X-α-Gal/AbA plate, indicating that the bait plasmid had no autoactivation activity. Furthermore, the colony size of the bait plasmid-transformed Y2HGold cells was similar to that of the empty pGBKT7 vector-transformed Y2HGold cells, suggesting that the bait plasmid was non-toxic to cells. Thus, the bait plasmid pGBKT7-BpLEAP-2 can be used in Y2H screening.

Construction of Y2H cDNA library of mudskipper MO/MΦ

We subsequently constructed a Y2H cDNA library of mudskipper MO/MΦ. The resultant prey library represented 2.8×10^6 independent clones with an estimated cDNA insert size ranging from 420 to 3 000 bp (average of 874 bp) (Figure 1). This result was similar to our previous work on ayu (Shi et al., 2011), indicating that the cDNA library can be used in Y2H screening.

Y2H screening against mudskipper MO/MΦ cDNA library using BpLEAP-2 as bait

Through high-stringency screening and subsequent confirmation by small-scale mating, 15 true positive clones were obtained from the mudskipper MO/MΦ cDNA expression library. The 15 prey plasmids were subsequently sequenced using the T7 primer. By sequence analysis, the redundant interactions were eliminated, and three unique interactions were confirmed. The corresponding prey proteins were mudskipper MOSPD2, DEAD-box helicase protein 41 (DDX41), and vav 3 guanine nucleotide exchange factor (VAV3). DDX41 is a member of the DEXDc helicase family, which was recently identified as an intracellular DNA sensor in myeloid dendritic cells (Zhang et al., 2011). VAV3 functions as an intracellular DNA sensor guanine nucleotide exchange factor (GEF) for members of the Rho family of small GTPases (Trenkle et al., 2000). MOSPD2 is a surface membrane protein associated with monocyte migration (Jiang et al., 2020; Mendel et al., 2017). Therefore, we selected *BpMOSPD2* as the target gene for further study.

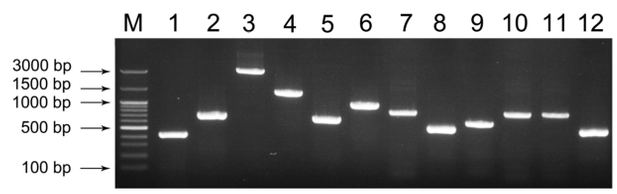

Figure 1 Insert size screening by PCR

Double-stranded cDNA amplicons were cloned into pGADT7-Rec vector using the Yeastmaker™ Yeast Transformation System 2 (Clontech). Twelve randomly selected colonies from the unamplified library were screened for size by PCR. PCR products (3 μL) were electrophoresed on 1% agarose/EtBr gel. Lane M: GeneRuler™ 1 kb DNA Ladder (0.5 μg).

Sequence characterization of *BpMOSPD2*

The complete cDNA sequence of *BpMOSPD2* was 2 268 nucleotides (nt) in length and comprised a large ORF of 1 578 nt, which was predicted to encode a 525 aa polypeptide with a calculated molecular weight (MW) of 59.87 kDa and an isoelectric point of 5.29. Multi-alignment of aa sequences showed that the fish MOSPD2 homologs were not only conserved in sequence but also in structure (Figure 2). The predicted BpMOSPD2 had the typical structure of MOSPD2 homologs, containing an N-terminal extracellular portion composed of a CRAL-TRIO domain (aa 100–242), a motile sperm domain (aa 332–446), a single-pass transmembrane domain (aa 498–520), and a short C-terminal intracellular domain (Figure 2).

Sequence comparison revealed that BpMOSPD2 shared more than 60.6% aa identity with other fish MOSPD2 homologs, with the highest aa identity of 84.6% for the white seabass (*Lates calcarifer*) homolog. Phylogenetic tree analysis indicated that BpMOSPD2 belonged to the fish MOSPD2 group and was most closely related to the Nile tilapia (*Oreochromis niloticus*) homolog (Figure 3).

Confirmation of BpLEAP-2/BpMOSPD2 interaction by Co-IP

The interaction between BpMOSPD2 and BpLEAP-2 was confirmed using the Co-IP assay in HEK293T cells overexpressing Myc-tagged-BpMOSPD2 and Flag-tagged-BpLEAP-2. Results showed that Myc-tagged-BpMOSPD2 and Flag-tagged-BpLEAP-2 were both expressed in HEK293T cells after co-transfection with pcDNA3.1-BpMOSPD2-Myc-His and pcDNA3.1-BpLEAP2-Flag-His, as reflected by their existence in the Co-IP supernatant (Figure 4A). Thus, a strong interaction existed between BpMOSPD2 and BpLEAP-2 (Figure 4A).

Preparation of rBpMOSPD2 and corresponding polyclonal antibody

The recombinant protein rBpMOSPD2 was overexpressed in *E. coli*. SDS-PAGE revealed that the MW of rBpMOSPD2 was approximately 65.6 kDa, similar to that calculated from the sequence (59.87 kDa BpMOSPD2 plus 5.73 kDa His-tag) (Figure 4B, lane 2). Subsequently, rBpMOSPD2 was purified using a Ni-NTA column (Figure 4B, lane 3) to prepare the polyclonal antibody (anti-BpMOSPD2) in mice. Western blotting was used to test the specificity of anti-BpMOSPD2. Results showed that anti-BpMOSPD2 was capable of specifically recognizing native BpMOSPD2 in mudskipper

MO/MΦ (Figure 4C, lane 5) and purified rBpMOSPD2 (Figure 4C, lane 6). The MW of native BpMOSPD2 was nearly 60 kDa, similar to that predicted from the gene sequence (Figure 4C, lane 5).

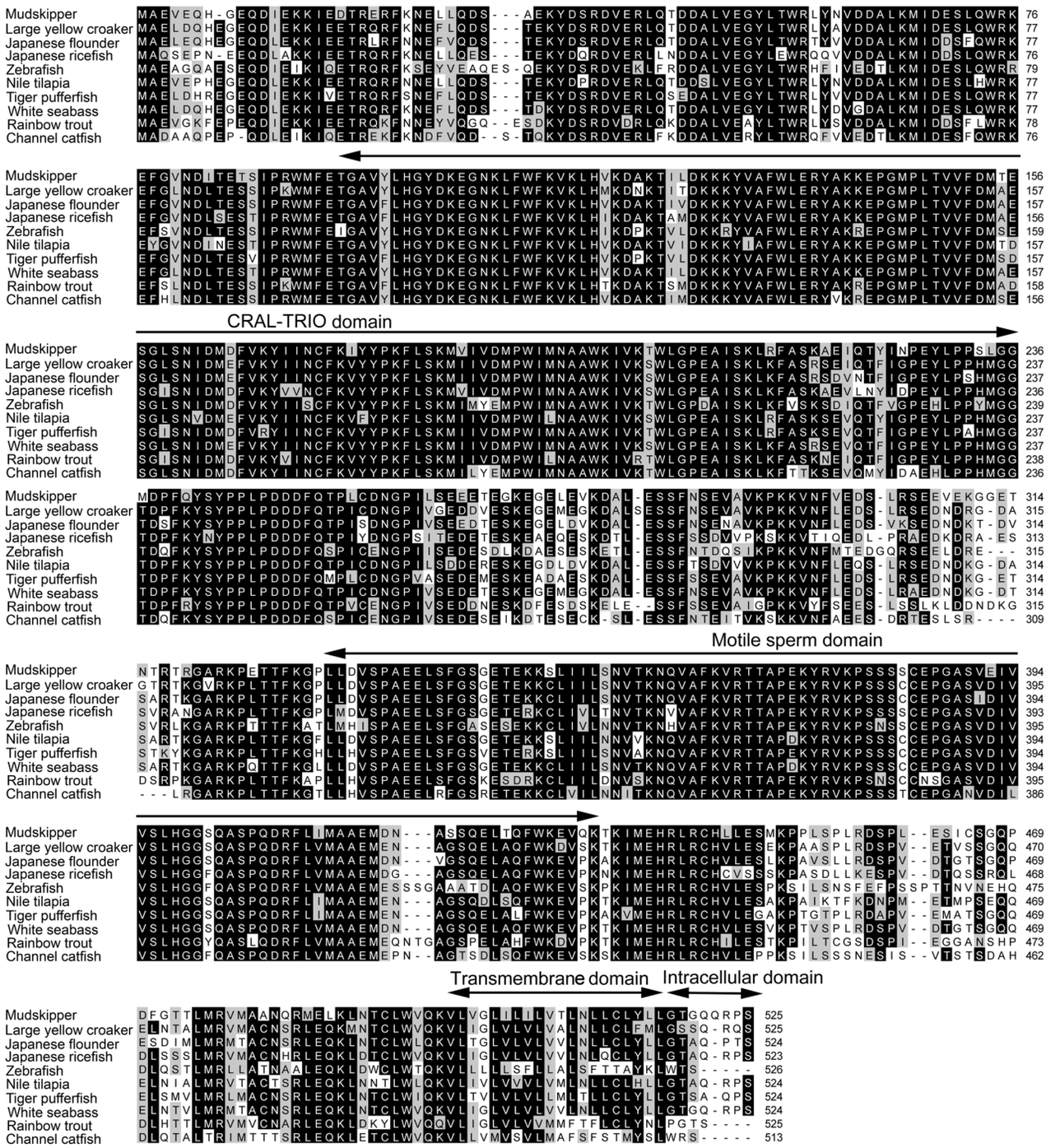

Figure 2 Multiple alignments of amino acid sequences of mudskipper and related fish MOSPD2 sequences

Threshold for shading was 70%; similar residues are marked in gray shadow, identical residues are marked in black shadow, and alignment gaps are marked with "-". CRAL-TRIO domain, motile sperm domain, transmembrane domain, and C-terminal intracellular domain are indicated above alignment. GenBank accession Nos. of the sequences are listed in Supplementary Table S1.

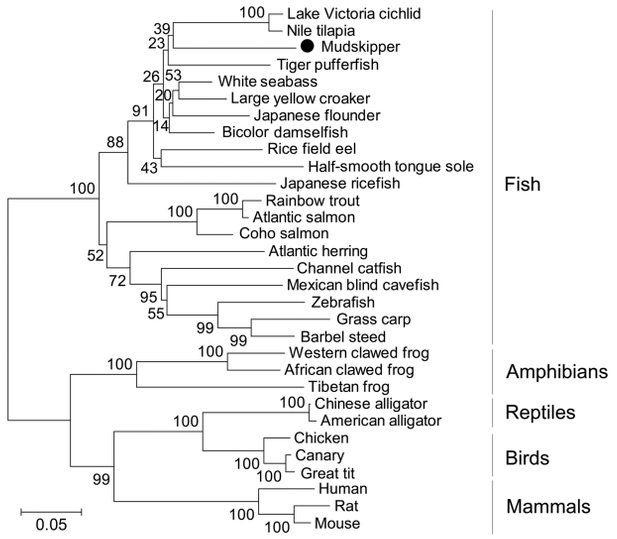

Figure 3 Phylogenetic (neighbor-joining) analysis of complete amino acid sequences of MOSPD2 using MEGA7.0

Values at forks indicate percentage of trees in which this grouping occurred after bootstrapping (1 000 replicates, shown only when >60%). Scale bar shows number of substitutions per base. GenBank accession Nos. of the sequences are listed in Supplementary Table S1.

Efficiency of *BpMOSPD2* knockdown by siRNA treatment

RNA interference was performed to knock down *BpMOSPD2* expression in mudskipper MO/MΦ *in vitro*. Compared with the normal control cells, the mRNA and protein levels of *BpMOSPD2* in *BpMOSPD2* siRNA-transfected cells decreased to 0.11-fold and 0.25-fold, respectively, while the scrambled siRNA-transfected group exhibited no significant changes in *BpMOSPD2* expression (Figure 4D, E), indicating that BpMOSPD2 could be knocked down effectively in mudskipper MO/MΦ by *BpMOSPD2* siRNA treatment.

BpMOSPD2 mediates BpLEAP-2-induced chemotaxis of mudskipper MO/MΦ

After transfection with scrambled siRNA, approximately 15.63% of MO/MΦ cells migrated to the lower chamber containing 10.0 μg/mL BpLEAP-2, whereas only 5.87% of cells migrated to the lower chamber without BpLEAP-2 (Figure 4F). On the other hand, after transfection with *BpMOSPD2* siRNA, only 6.0% of MO/MΦ cells migrated to the lower chamber containing 10.0 μg/mL BpLEAP-2, similar to that of without BpLEAP-2 (Figure 4F). In the no siRNA-treated group, the cell migration percentages in the BpLEAP-2-untreated and -treated groups were 5.01% and 15.96%, respectively. This suggests that the effect of BpLEAP-2 on mudskipper MO/MΦ migration was efficaciously inhibited by *BpMOSPD2* knockdown.

BpMOSPD2 mediates effect of BpLEAP-2 on bacterial killing activity of mudskipper MO/MΦ

After MO/MΦ transfection with siRNA, the survival rate of the bacteria was investigated via direct measurement of intracellular live *E. tarda* CFUs in mudskipper MO/MΦ. When mudskipper MO/MΦ were transfected with scrambled siRNA, the survival rate of *E. tarda* was 82.22% in the BpLEAP-2-untreated group, whereas the survival rate was 29.98% in the BpLEAP-2-treated group (Figure 5A, B). When mudskipper MO/MΦ were transfected with *BpMOSPD2* siRNA, the survival rate of *E. tarda* was 77.81% in the BpLEAP-2-untreated group and 70.51% in the BpLEAP-2-treated group (Figure 5A, B). The survival rates of *E. tarda* in the no siRNA-treated MO/MΦ were 83.83% and 29.23% in the BpLEAP-2-untreated and -treated groups, respectively. This indicated that the BpLEAP-2-enhanced bacterial killing effects on mudskipper MO/MΦ were eliminated after *BpMOSPD2* knockdown.

BpMOSPD2 mediates BpLEAP-2 effect on cytokine mRNA expression in mudskipper MO/MΦ

In our previous study, BpLEAP-2 was found to alter cytokine mRNA expression in mudskipper MO/MΦ (Chen et al., 2016), so we investigated whether BpMOSPD2 mediates the effect of BpLEAP-2 on MO/MΦ cytokine expression. Without BpLEAP-2 treatment, mRNA expression of tested cytokines in mudskipper MO/MΦ treated with scrambled siRNA or *BpMOSPD2* siRNA did not change significantly when compared to that in the no siRNA-treated group (Figure 5C, F). BpLEAP-2 treatment significantly decreased mRNA expression of proinflammatory cytokines (*BpTNFα* and *BpIL-1β*) in mudskipper MO/MΦ treated with scrambled siRNA or no siRNA and increased mRNA expression of anti-inflammatory cytokines (*BpIL-10* and *BpTGFβ*). However, *BpMOSPD2* knockdown weakened this effect of BpLEAP-2 on mudskipper MO/MΦ (Figure 5C, F).

DISCUSSION

LEAP-2 is a typical antimicrobial peptide present in vertebrates (Chen et al., 2019; Howard et al., 2010; Li et al., 2014, 2015b; Townes et al., 2004). In teleosts, LEAP-2 exhibits direct antimicrobial activity against a wide range of microorganisms (Bo et al., 2019; Chen et al., 2019; Li et al., 2014, 2015b; Liu et al., 2020). Interestingly, we recently found that BpLEAP-2 protects mudskippers against *E. tarda* not by direct antimicrobial activity but by its immunomodulatory function on MO/MΦ (Chen et al., 2016). To date, however, no immune-related receptors have been identified for LEAP-2. Therefore, we investigated the mechanism by which BpLEAP-2 acts on mudskipper MO/MΦ. In this study, we used Y2H cDNA library screening to identify the putative receptor(s) of BpLEAP-2 in mudskipper MO/MΦ, and the gene encoding BpMOSPD2 was screened out. Sequence analysis revealed that BpMOSPD2 was a single-transmembrane protein with a C-terminal tail in cytoplasm, similar to other homologs (Di Mattia et al., 2018; Jiang et al., 2020; Mendel et al., 2017). The interaction between BpMOSPD2 and BpLEAP-2 was confirmed by Co-IP assay.

MOSPD2, as a major sperm protein (MSP) domain-containing protein (Mendel et al., 2017), is a single-pass membrane protein, though information on its functions is

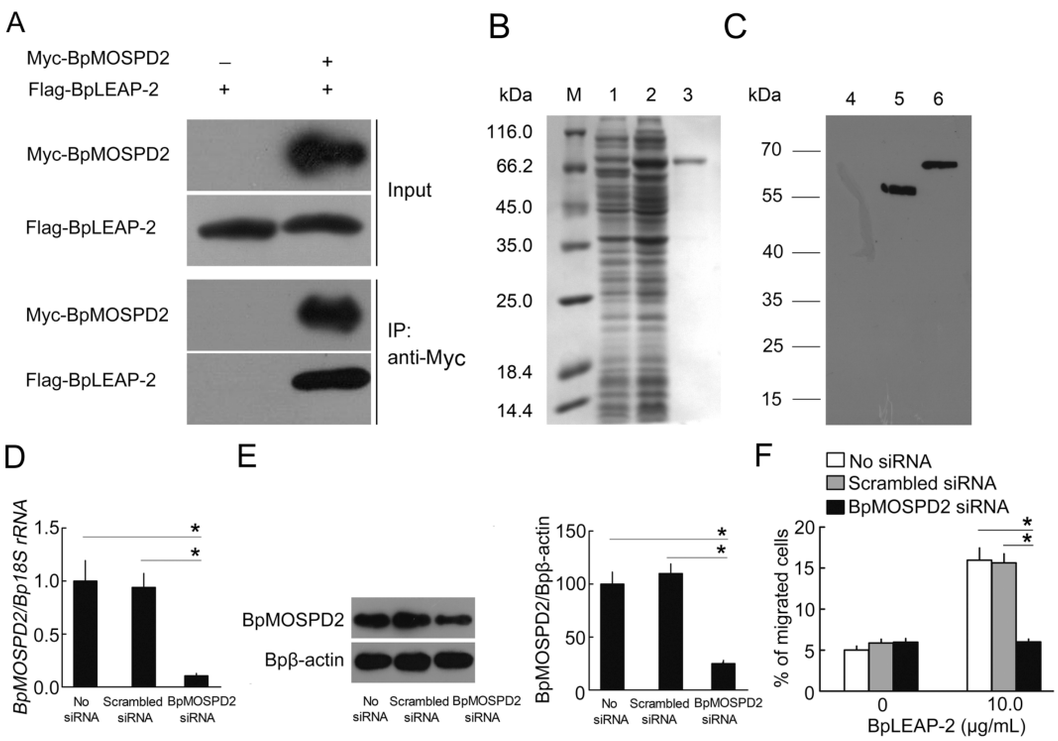

Figure 4 BpMOSPD2 mediates BpLEAP-2-induced chemotaxis of mudskipper MO/MΦ

A: Interaction potential between BpMOSPD2 and BpLEAP-2 through Co-IP assay. HEK293T cells were co-transfected with pcDNA3.1-BpMOSPD2-Myc-His and pcDNA3.1-BpLEAP2-Flag-His. Co-transfection was followed by immunoprecipitation with Myc Tag mAb and detection by Flag Tag mAb. "+" means corresponding plasmid was transfected. "–" means corresponding plasmid was not transfected. Input: Input control. Myc-BpMOSPD2: Myc-tagged-BpMOSPD2. Flag-BpLEAP-2: Flag-tagged-BpLEAP-2. B: SDS-PAGE analysis of BpMOSPD2 overexpressed in *E. coli* cells. Lane M: protein marker; 1 and 2: protein from BL21 (DE3) transformed with pET-30a-BpMOSPD2 plasmid before and after IPTG induction, respectively; 3: purified recombinant protein. C: Western blot analysis of BpMOSPD2. Lane 4: protein from BL21 (DE3) transformed with pET-30a-BpMOSPD2 plasmid before IPTG induction, negative control; Lane 5: total proteins of mudskipper MO/MΦ; Lane 6: purified recombinant protein. D: qRT-PCR analysis of *BpMOSPD2* mRNA expression level in mudskipper MO/MΦ following scrambled or *BpMOSPD2* siRNA treatment. *BpMOSPD2* transcript was normalized to *Bp18S rRNA*. Data are expressed as mean±*SD*. n=4. *: P<0.05. E: Western blot analysis of BpMOSPD2 level in mudskipper MO/MΦ following scrambled or *BpMOSPD2* siRNA treatment. Bpβ-actin was used as an endogenous control. Histogram showing changes in relative protein band intensity of BpMOSPD2 following siRNA treatment. Data are expressed as mean±*SD*. n=4. *: P<0.05. G: BpMOSPD2 mediated BpLEAP-2-induced chemotaxis of mudskipper MO/MΦ. MO/MΦ cells were transfected with *BpMOSPD2* siRNA for 72 h, and scrambled siRNA-treated groups were used as a control. Cells were then resuspended in RPMI 1640 supplemented with 10% FBS and added to upper chamber. BpLEAP-2 was added to lower chamber at a dose of 0 or 10.0 μg/mL. After incubation at 24 °C for 4 h, cells were viewed under a light microscope, and percentage of cells that migrated to the lower chamber was calculated. Data are expressed as mean±*SD*. n=4. *: P<0.05.

limited. MOSPD2 is a potential regulator of monocyte and neutrophil migration (Mendel et al., 2017; Jiang et al., 2020), and anti-MOSPD2 monoclonal antibodies are reported to constitute a potential therapy for the treatment of central nervous system inflammatory diseases (Yacov et al., 2020). MOSPD2 also plays a key role in the migration and metastasis of breast cancer cells (Salem et al., 2019). Moreover, MOSPD2 is a novel tethering component related to vesicle-associated membrane protein-associated proteins (VAP), bridging the endoplasmic reticulum (ER) with a variety of distinct organelles (Di Mattia et al., 2018).

Some HDPs, such as cathelicidins and β-defensins, are reported to induce chemotaxis through interactions with their receptors (Li et al., 2015a; Röhrl et al., 2008, 2010; Tjabringa et al., 2006). For example, our previous study showed that P2X7R mediates cathelicidin-induced chemotaxis of ayu MO/MΦ (Li et al., 2015a). BpLEAP-2 induces the migration of mudskipper MO/MΦ in a dose- and time-dependent manner (Chen et al., 2016). Given that BpMOSPD2 is a putative receptor of BpLEAP-2 in mudskipper MO/MΦ, we investigated whether BpMOSPD2 mediates BpLEAP-2-dependent chemotaxis of mudskipper MO/MΦ. By *BpMOSPD2* knockdown in mudskipper MO/MΦ, we found that BpLEAP-2-induced MO/MΦ chemotaxis was significantly inhibited, suggesting that BpLEAP-2-induced chemotaxis of mudskipper MO/MΦ is BpMOSPD2-dependent. Nevertheless, previous study has shown that silencing or neutralizing MOSPD2 in human monocytes and neutrophils restricts their migration

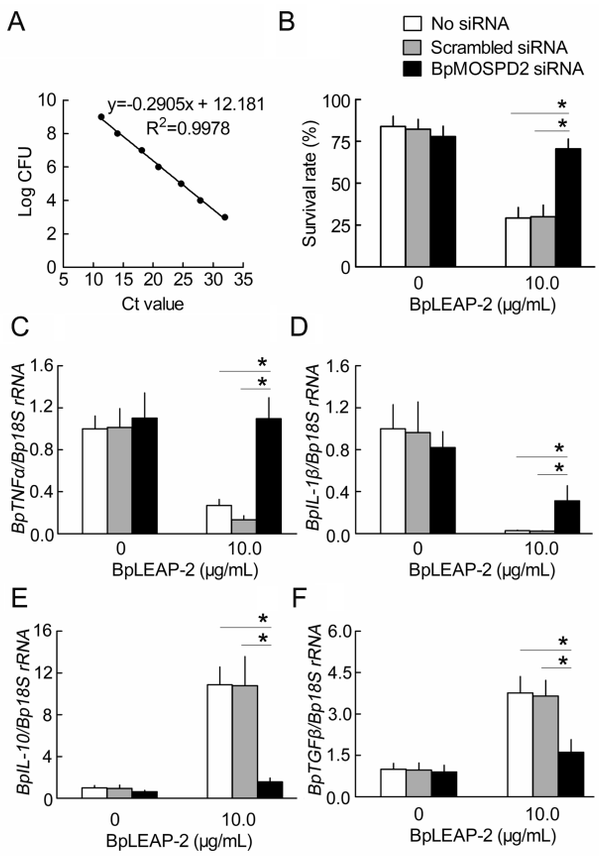

Figure 5 BpMOSPD2 mediates BpLEAP-2 effect on bacterial killing ability and cytokine mRNA expression in mudskipper MO/MΦ

A: Standard curve was generated by qRT-PCR detection of 10-fold serial dilutions of *E. tarda*. B: MO/MΦ cells were transfected with scrambled siRNA or *BpMOSPD2* siRNA for 72 h, and then treated with 0 or 10.0 μg/mL BpLEAP-2 for another 8 h. Live *E. tarda* bacteria were added at an MOI of 10 and incubated for an additional 30 min. Killing of *E. tarda* by MO/MΦ was measured via CFU assay. qRT-PCR was used for quantification of *E. tarda* in mudskipper MO/MΦ based on the above standard curve. Histogram representing BpLEAP-2 effect on bacterial killing ability of mudskipper MO/MΦ upon *BpMOSPD2* knockdown. Each bar represents mean±*SD*. *n*=4. *: *P*<0.05. C–F: MO/MΦ cells were transfected with scrambled siRNA or *BpMOSPD2* siRNA for 72 h and then treated with 0 or 10.0 μg/mL BpLEAP-2 for another 8 h. Cells were then washed with sterile PBS and infected with live *E. tarda* at an MOI of 10. Cells were collected at 8 h after BpLEAP-2 treatment. mRNA expression levels of *BpTNFα* (C), *BpIL-1β* (D), *BpIL-10* (E), and *BpTGFβ* (F) were normalized to expression of *Bp18S* rRNA. Each bar represents mean±*SD*. *n*=4. *: *P*<0.05.

when induced by different chemokines, including CXC motif chemokine ligand 12, CC motif chemokine ligand 5, monocyte chemoattractant protein-1 (MCP-1) and macrophage inflammatory protein-3 (MIP-3) (Mendel et al., 2017). These authors speculated that MOSPD2 might alternatively pair with chemokine receptors or other surface membrane proteins to serve as a co-receptor in a complex necessary for full activation of chemokine receptors; however, this assumption has not yet been confirmed. Based on our results, BpLEAP-2 most likely induced the chemotaxis of mudskipper MO/MΦ via BpMOSPD2 directly.

Aside from inducing chemotaxis, HDPs also possess immunomodulatory functions on immunocytes (Elssner et al., 2004; Li et al., 2015a; Wu et al., 2018; Zhou et al., 2020). For example, ayu cathelicidin promotes MO/MΦ phagocytosis, intracellular bacterial killing, and inflammatory cytokine expression via mediation of P2X7R (Li et al., 2015a). Our previous study showed that BpLEAP-2 significantly increases the bacterial killing capability in mudskipper MO/MΦ but does not affect phagocytosis (Chen et al., 2016). Moreover, BpLEAP-2 decreases *E. tarda*-induced *BpTNFα* and *BpIL-1β* mRNA expression in MO/MΦ, suggesting that BpLEAP-2 may play a role in preventing the exaggeration of fish pro-inflammatory immune response caused by *E. tarda* infection (Chen et al., 2016). In this study, after *BpMOSPD2* knockdown in mudskipper MO/MΦ, the BpLEAP-2-enhanced bacterial killing effect on mudskipper MO/MΦ was eliminated, suggesting that BpMOSPD2 mediates the intracellular *E. tarda* killing capacity of BpLEAP-2. Knockdown of *BpMOSPD2* expression inhibited the effect of BpLEAP-2 on mRNA expression of *BpIL-10*, *BpTNFα*, *BpIL-1β*, and *BpTGFβ* in MO/MΦ, revealing that the effect of BpLEAP-2 on cytokine production is also BpMOSPD2-dependent.

In summary, BpMOSPD2 was identified to interact with BpLEAP-2 *in vivo* for the first time. Knockdown of *BpMOSPD2* expression not only eliminated the effects of BpLEAP-2 on the chemotaxis of mudskipper MO/MΦ, but also weakened its effects on intracellular bacterial killing and cytokine mRNA expression in MO/MΦ. This work broadens our knowledge on the functions and mechanisms of fish HDPs, and the results could be used as a reference in controlling various fish diseases.

SUPPLEMENTARY DATA

Supplementary data to this article can be found online.

COMPETING INTERESTS

The authors declare that they have no competing interests.

AUTHORS' CONTRIBUTIONS

J.C. (Jiong Chen) drafted the experiments; C.H.L., J.C. (Jie Chen), and L.N. performed the experiments. J.C. (Jiong Chen) and C.H.L. analyzed the data and wrote the paper. All authors read and approved the final version of the manuscript.

REFERENCES

Bąbolewska E, Brzezińska-Błaszczyk E. 2015. Human-derived cathelicidin LL-37 directly activates mast cells to proinflammatory mediator synthesis and migratory response. *Cellular Immunology*, **293**(2): 67−73.

Barrile F, M'Kadmi C, De Francesco PN, Cabral A, Romero GG, Mustafá ER, et al. 2019. Development of a novel fluorescent ligand of growth hormone secretagogue receptor based on the N-Terminal Leap2 region. *Molecular and Cellular Endocrinology*, **498**: 110573.

Bo J, Yang Y, Zheng RH, Fang C, Jiang YL, Liu J, et al. 2019. Antimicrobial activity and mechanisms of multiple antimicrobial peptides isolated from rockfish *Sebastiscus marmoratus*. *Fish & Shellfish Immunology*, **93**: 1007−1017.

Brogden KA. 2005. Antimicrobial peptides: pore formers or metabolic inhibitors in bacteria?. *Nature Reviews Microbiology*, **3**(3): 238−250.

Brown KL, Hancock REW. 2006. Cationic host defense (antimicrobial) peptides. *Current Opinion in Immunology*, **18**(1): 24−30.

Chen J, Chen Q, Lu XJ, Chen J. 2016. The protection effect of LEAP-2 on the mudskipper (*Boleophthalmus pectinirostris*) against *Edwardsiella tarda* infection is associated with its immunomodulatory activity on monocytes/macrophages. *Fish & Shellfish Immunology*, **59**: 66−76.

Chen J, Lv YP, Dai QM, Hu ZH, Liu ZM, Li JH. 2019. Host defense peptide LEAP-2 contributes to monocyte/macrophage polarization in barbel steed (*Hemibarbus labeo*). *Fish & Shellfish Immunology*, **87**: 184−192.

Chen J, Nie L, Chen J. 2018. Mudskipper (*Boleophthalmus pectinirostris*) hepcidin-1 and hepcidin-2 present different gene expression profile and antibacterial activity and possess distinct protective effect against *Edwardsiella tarda* infection. *Probiotics and Antimicrobial Proteins*, **10**(2): 176−185.

Di Mattia T, Wilhelm LP, Ikhlef S, Wendling C, Spehner D, Nominé Y, et al. 2018. Identification of MOSPD2, a novel scaffold for endoplasmic reticulum membrane contact sites. *EMBO Reports*, **19**(7): e45453.

Ding FF, Li CH, Chen J. 2019. Molecular characterization of the NK-lysin in a teleost fish, *Boleophthalmus pectinirostris*: antimicrobial activity and immunomodulatory activity on monocytes/macrophages. *Fish & Shellfish Immunology*, **92**: 256−264.

Elssner A, Duncan M, Gavrilin M, Wewers MD. 2004. A novel $P2X_7$ receptor activator, the human cathelicidin-derived peptide LL37, induces IL-1β processing and release. *The Journal of Immunology*, **172**(8): 4987−4994.

Fabisiak A, Murawska N, Fichna J. 2016. LL-37: cathelicidin-related antimicrobial peptide with pleiotropic activity. *Pharmacological Reports*, **68**(4): 802−808.

Fruitwala S, El-Naccache DW, Chang TL. 2019. Multifaceted immune functions of human defensins and underlying mechanisms. *Seminars in Cell & Developmental Biology*, **88**: 163−172.

Ge XC, Yang H, Bednarek MA, Galon-Tilleman H, Chen PR, Chen M, et al. 2018. LEAP2 is an endogenous antagonist of the ghrelin receptor. *Cell Metabolism*, **27**(2): 461−469.

Guan F, Lu XJ, Li CH, Chen J. 2017. Molecular characterization of mudskipper (*Boleophthalmus pectinirostris*) hypoxia-inducible factor-1α (HIF-1α) and analysis of its function in monocytes/macrophages. *PLoS One*, **12**(5): e0177960.

Gupta K, Subramanian H, Ali H. 2016. Modulation of host defense peptide-mediated human mast cell activation by LPS. *Innate Immunity*, **22**(1): 21−30.

Hale JDF, Hancock REW. 2007. Alternative mechanisms of action of cationic antimicrobial peptides on bacteria. *Expert Review of Anti-infective Therapy*, **5**(6): 951−959.

Hancock REW, Haney EF, Gill EE. 2016. The immunology of host defence peptides: Beyond antimicrobial activity. *Nature Reviews Immunology*, **16**(5): 321−334.

Hancock REW, Nijnik A, Philpott DJ. 2012. Modulating immunity as a therapy for bacterial infections. *Nature Reviews Microbiology*, **10**(4): 243−254.

Howard A, Townes C, Milona P, Nile CJ, Michailidis G, Hall J. 2010. Expression and functional analyses of liver expressed antimicrobial peptide-2 (LEAP-2) variant forms in human tissues. *Cellular Immunology*, **261**(2): 128−133.

Jiang W, Chen J, Guo ZP, Zhang L, Chen GP. 2020. Molecular characterization of a MOSPD2 homolog in the barbel steed (*Hemibarbus labeo*) and its involvement in monocyte/macrophage and neutrophil migration. *Molecular Immunology*, **119**: 8−17.

Krause A, Sillard R, Kleemeier B, Klüver E, Maronde E, Conejo-García JR, et al. 2003. Isolation and biochemical characterization of LEAP-2, a novel blood peptide expressed in the liver. *Protein Science*, **12**(1): 143−152.

Kumar S, Stecher G, Tamura K. 2016. MEGA7: molecular evolutionary genetics analysis version 7.0 for bigger datasets. *Molecular Biology and Evolution*, **33**(7): 1870−1874.

Li CH, Lu XJ, Li MY, Chen J. 2015a. Cathelicidin modulates the function of monocytes/macrophages via the P2X7 receptor in a teleost, *Plecoglossus altivelis*. *Fish & Shellfish Immunology*, **47**(2): 878−885.

Li HX, Lu XJ, Li CH, Chen J. 2014. Molecular characterization and functional analysis of two distinct liver-expressed antimicrobial peptide 2 (LEAP-2) genes in large yellow croaker (*Larimichthys crocea*). *Fish & Shellfish Immunology*, **38**(2): 330−339.

Li HX, Lu XJ, Li CH, Chen J. 2015b. Molecular characterization of the liver-expressed antimicrobial peptide 2 (LEAP-2) in a teleost fish, *Plecoglossus altivelis*: antimicrobial activity and molecular mechanism. *Molecular Immunology*, **65**(2): 406−415.

Liu B, Liu GD, Guo HY, Zhu KC, Guo L, Zhang N, et al. 2020. Characterization and functional analysis of liver-expressed antimicrobial peptide-2 (LEAP-2) from golden pompano *Trachinotus ovatus* (Linnaeus 1758). *Fish & Shellfish Immunology*, **104**: 419−430.

Liu TX, Gao YH, Wang RX, Xu TJ. 2014. Characterization, evolution and functional analysis of the liver-expressed antimicrobial peptide 2 (LEAP-2) gene in miiuy croaker. *Fish & Shellfish Immunology*, **41**(2): 191−199.

Livak KJ, Schmittgen TD. 2001. Analysis of relative gene expression data using real-time quantitative PCR and the $2^{-\Delta\Delta C_T}$ method. *Methods*, **25**(4): 402−408.

Lu XJ, Chen J, Huang ZA, Shi YH, Lü JN. 2011. Identification and characterization of a novel cathelicidin from ayu, *Plecoglossus altivelis*. *Fish & Shellfish Immunology*, **31**(1): 52−57.

Luo SW, Luo KK, Liu SJ. 2020. A novel LEAP-2 in diploid hybrid fish (*Carassius auratus cuvieri* ♀ × *Carassius auratus* red var. ♂) confers protection against bacteria-stimulated inflammatory response. *Comparative Biochemistry and Physiology Part C: Toxicology & Pharmacology*, **228**: 108665.

Mendel I, Yacov N, Salem Y, Propheta-Meiran O, Ishai E, Breitbart E. 2017. Identification of motile sperm domain-containing protein 2 as regulator of human monocyte migration. *The Journal of Immunology*, **198**(5): 2125−2132.

Nagaoka I, Tamura H, Hirata M. 2006. An antimicrobial cathelicidin peptide, human CAP18/LL-37, suppresses neutrophil apoptosis via the activation of

formyl-peptide receptor-like 1 and $P2X_7$. *The Journal of Immunology*, **176**(5): 3044−3052.

Rajanbabu V, Chen JY. 2011. The antimicrobial peptide, tilapia hepcidin 2-3, and PMA differentially regulate the protein kinase C isoforms, TNF-α and COX-2, in mouse RAW264.7 macrophages. *Peptides*, **32**(2): 333−341.

Ren Y, Liu SF, Nie L, Cai SY, Chen J. 2019. Involvement of ayu NOD2 in NF-κB and MAPK signaling pathways: insights into functional conservation of NOD2 in antibacterial innate immunity. *Zoological Research*, **40**(2): 77−88.

Röhrl J, Yang D, Oppenheim JJ, Hehlgans T. 2008. Identification and biological characterization of mouse β-defensin 14, the orthologue of human β-defensin 3. *The Journal of Biological Chemistry*, **283**(9): 5414−5419.

Röhrl J, Yang D, Oppenheim JJ, Hehlgans T. 2010. Human β-defensin 2 and 3 and their mouse orthologs induce chemotaxis through interaction with CCR2. *The Journal of Immunology*, **184**(12): 6688−6694.

Salem Y, Yacov N, Propheta-Meiran O, Breitbart E, Mendel I. 2019. Newly characterized motile sperm domain-containing protein 2 promotes human breast cancer metastasis. *International Journal of Cancer*, **144**(1): 125−135.

Scott MG, Davidson DJ, Gold MR, Bowdish D, Hancock RE. 2002. The human antimicrobial peptide LL-37 is a multifunctional modulator of innate immune responses. *The Journal of Immunology*, **169**(7): 3883−3891.

Shata MTM, Abdel-Hameed EA, Hetta HF, Sherman KE. 2013. Immune activation in HIV/HCV-infected patients is associated with low-level expression of liver expressed antimicrobial peptide-2 (LEAP-2). *Journal of Clinical Pathology*, **66**(11): 967−975.

Shen HY, Zhou Y, Zhou QJ, Li MY, Chen J. 2020. Mudskipper interleukin-34 modulates the functions of monocytes/macrophages via the colony-stimulating factor-1 receptor 1. *Zoological Research*, **41**(2): 123−137.

Shi YH, Chen J, Li CH, Yang HY, Lu XJ. 2011. The establishment of a library screening method based on Yeast Two-Hybrid system and its use to determine the potential interactions of liver proteins in ayu, *Plecoglossus altivelis*. *Fish & Shellfish Immunology*, **30**(4-5): 1184−1187.

Subramanian H, Gupta K, Guo Q, Price R, Ali H. 2011. Mas-related gene X2 (MrgX2) is a novel G protein-coupled receptor for the antimicrobial peptide LL-37 in human mast cells: resistance to receptor phosphorylation, desensitization, and internalization. *Journal of Biological Chemistry*, **286**(52): 44739−44749.

Tjabringa GS, Ninaber DK, Drijfhout JW, Rabe KF, Hiemstra PS. 2006. Human cathelicidin LL-37 is a chemoattractant for eosinophils and neutrophils that acts via formyl-peptide receptors. *International Archives of Allergy and Immunology*, **140**(2): 103−112.

Townes CL, Michailidis G, Nile CJ, Hall J. 2004. Induction of cationic chicken liver-expressed antimicrobial peptide 2 in response to *Salmonella enterica* infection. *Infection and Immunity*, **72**(12): 6987−6993.

Trenkle T, McClelland M, Adlkofer K, Welsh J. 2000. Major transcript variants of VAV3, a new member of the VAV family of guanine nucleotide exchange factors. *Gene*, **245**(1): 139−149.

Vandamme D, Landuyt B, Luyten W, Schoofs L. 2012. A comprehensive summary of LL-37, the factotum human cathelicidin peptide. *Cellular Immunology*, **280**(1): 22−35.

Wang YP, Lu Y, Zhang Y, Ning ZM, Li Y, Zhao Q, et al. 2015. The draft genome of the grass carp (*Ctenopharyngodon idellus*) provides insights into its evolution and vegetarian adaptation. *Nature Genetics*, **47**(6): 625−631.

Wu YJ, Li DD, Wang Y, Liu X, Zhang YQ, Qu WT, et al. 2018. Beta-defensin 2 and 3 promote bacterial clearance of *Pseudomonas aeruginosa* by inhibiting macrophage autophagy through downregulation of early growth response gene-1 and c-FOS. *Frontiers in Immunology*, **9**: 211.

Yacov N, Kafri P, Salem Y, Propheta-Meiran O, Feldman B, Breitbart E, et al. 2020. MOSPD2 is a therapeutic target for the treatment of CNS inflammation. *Clinical & Experimental Immunology*, **201**(2): 105−120.

Yang J, Lu XJ, Chai FC, Chen J. 2016. Molecular characterization and functional analysis of a piscidin gene in large yellow croaker (*Larimichthys crocea*). *Zoological Research*, **37**(6): 347−355.

Zahran E, Risha E, Elbahnaswy S, Mahgoub HA, El-Moaty AA. 2019. Tilapia piscidin 4 (TP4) enhances immune response, antioxidant activity, intestinal health and protection against *Streptococcus iniae* infection in Nile tilapia. *Aquaculture*, **513**: 734451.

Zhang ZQ, Yuan B, Bao MS, Lu N, Kim T, Liu YJ. 2011. The helicase DDX41 senses intracellular DNA mediated by the adaptor STING in dendritic cells. *Nature Immunology*, **12**(10): 959−965.

Zhou Y, Zhou QJ, Qiao Y, Chen J, Li MY. 2020. The host defense peptide β-defensin confers protection against *Vibrio anguillarum* in ayu, *Plecoglossus altivelis*. *Developmental & Comparative Immunology*, **103**: 103511.

Zhu JY, Wang H, Wang J, Wang XL, Peng S, Geng Y, et al. 2017. Identification and characterization of a β-defensin gene involved in the immune defense response of channel catfish, *Ictalurus punctatus*. *Molecular Immunology*, **85**: 256−264.